Taylor & Francis
Taylor & Francis Group

Desalination at low temperatures: an exergy analysis

Veera Gnaneswar Gude[a,*], Nagamany Nirmalakhandan[b], Shuguang Deng[c], Anand Maganti[d]

[a]*Civil & Environmental Engineering Department, Mississippi State University 235G Walker Hall,*
Box 9546, Mississippi State, MS 39762, USA
Tel. +662 325 0345; Fax: +662 325 7189; email: gude@cee.msstate.edu
[b]*Civil Engineering Department, New Mexico State University, Las Cruces, NM 88003, USA*
[c]*Chemical Engineering Department, New Mexico State University, Las Cruces, NM 88003, USA*
[d]*Department of Transportation, 703 B Street, Marysville, CA 95901, USA*

ABSTRACT

A new low-temperature phase-change desalination process has been presented where saline water is desalinated by evaporation at near-ambient temperatures under low pressures. The low pressure is achieved naturally in the head space of water columns of a height equal to the local barometric head. By connecting the head space of such a saline water column to that of a distilled water column, and by maintaining the temperature of the former about 15–20°C above that of the latter, fresh water is evaporated from the saline column and condensed in the distilled water column. This paper presents an exergy analysis of this process to evaluate the thermodynamic efficiency of its major components and to identify suitable operating conditions to minimize exergy destruction. Three different heat sources such as direct solar, photovoltaic energy as well as a low grade heat source were considered. It was found that the major exergy destruction occurs in the condenser where the latent heat of the water vapor is lost to the environment. Exergy performance of individual process components and recommendations to further improve the exergy efficiency of the proposed process are presented.

Keywords: Desalination; Energy; Exergy analysis; Second law of thermodynamics; Exergy destruction; Irreversibility

1. Introduction

Desalination has now become a promising alternative to freshwater supply due to rapidly increasing demands for freshwater throughout the world. However, since common desalination technologies including thermal and membrane processes demand large quantities of energy, providing desalinated water can place a concomitant demand on the limited energy sources [1]. Since energy production involves degradation of environmental quality; water, energy, and environmental issues are the most immediate concerns of the world [2].

Thermal technologies (multi stage flash distillation – MSF, multi effect distillation – MED and mechanical vapor compression – MVC) require energy in the form of heat while membrane technologies require electrical energy to produce freshwater. Although, energy consumption in the desalination technologies has been lowered significantly over the past two decades, current global energy resources are still not adequate to support the desalination processes as the demand for freshwater on the global scale is expected to rise sharply.

Fortunately, water scarce regions around the world have high solar insolation rates which are suitable for thermal energy harvesting by solar collectors [3]. Direct solar energy can be utilized in the simplest configuration

---

of thermal desalination technology, known as, solar still (SS). However, SS are very inefficient in utilizing the solar energy due to accommodation of evaporating and condensing surfaces in a single glass roofed vessel. As a result several modifications to the SS design have been studied to increase its energy efficiency and product yield in single and multi-effect stills [4–6]. One of the configurations resulted in high distillate yields by separating the evaporation and condensing chambers. Energy efficiency of the SS can be further improved if they can be operated at lower temperatures in the 40–55°C as compared to the common range of 60–75°C [7,8].

A new low temperature desalination process was developed to reduce the heat losses from the evaporation chamber there by increasing the freshwater yield. This process operates under near vacuum pressures created by exploiting natural forces of gravity and barometric head as further explained in the next section. Results of a proof-of-concept study of this process configuration and the first law analysis of the process were reported in our previous publications [9–13].

The objective of this study is to evaluate sources of inefficiency in the process to identify operational parameters to maximize thermodynamic performance of this process and to develop process modifications. This evaluation is done through exergy analysis of the major components in the process. Energy and exergy analysis of low temperature desalination process utilizing direct solar energy, photovoltaic energy and a low grade heat source are presented.

2. Description of the low temperature desalination system

Physical principles behind the proposed low-temperature desalination process can be illustrated by considering two barometric columns at ambient temperature, one filled with freshwater and the other with saline water. The head space of these two columns will be occupied by the vapors of the respective fluids at their respective vapor pressures. Suppose these head spaces are connected to one another. Since the vapor pressure of freshwater is slightly higher than that of saline water at ambient temperature, water vapor will distill from the freshwater column into the saline water column. However, if the temperature of the saline water column is maintained slightly higher than that of the fresh water column to raise the vapor pressure of the saline water side above that of the fresh water side, water vapor from the saline water column will distill into the fresh water column. A temperature difference of about 15°C is adequate to overcome the vapor pressure difference to drive this distillation process. Such low temperature differences can be achieved using low grade heat sources

such as solar energy, waste process heat, thermal energy storage systems etc.

A schematic arrangement of a desalination system based on the above principles is shown in Fig. 1(a). Components of the desalination unit include an evaporation chamber (EC), a natural draft condenser (CON), a heat exchangers (HE), and three 10-m tall columns. These three columns serve as the saline water column; the brine withdrawal column; and the freshwater column, each with its own constant-level holding tank, SWT, BT, and FWT, respectively. These holding tanks are installed at the ground level while the EC is installed atop the saline water and brine withdrawal columns at the barometric height of about 10 m above the free surface in
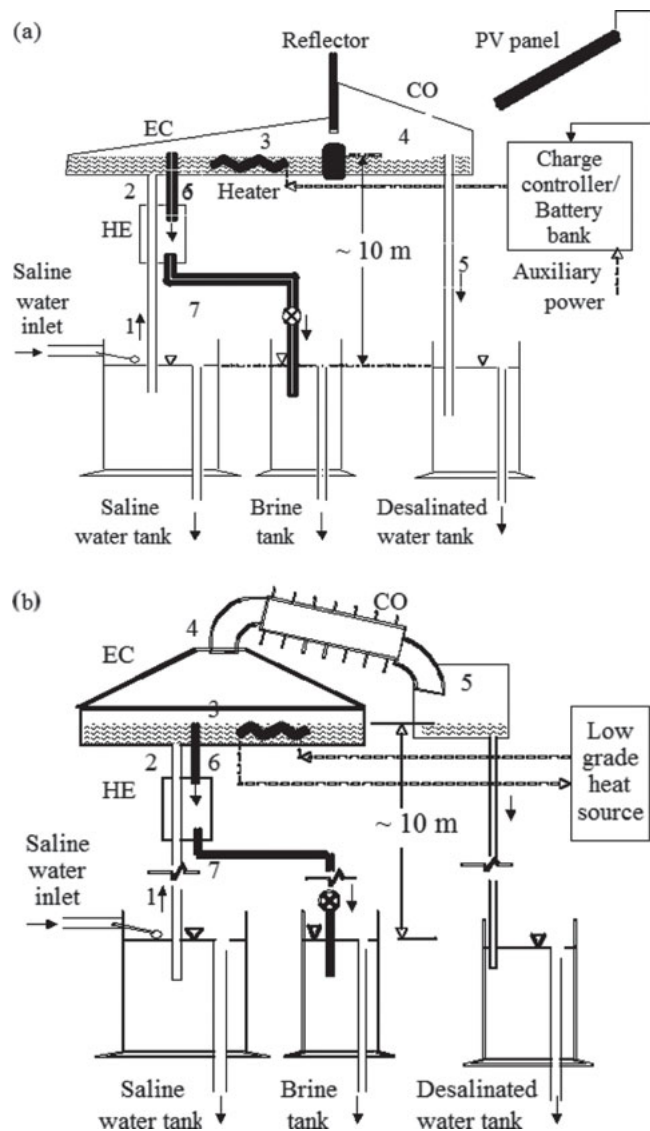

Fig. 1. Low temperature desalination system process configuration using (a) direct solar and photovoltaic energy; (b) low grade heat source.

the holding tanks to create a Torricelli's vacuum in the head space of the EC. The top of the EC is exposed to sunlight in a configuration where direct solar energy is utilized for evaporation as shown in Fig. 1(a). The top of the freshwater column is connected to the outlet of the condenser. When the temperature of the saline water in the EC is increased by about 15–20°C above the ambient temperature, water vapor will flow from the EC to the CON where it will condense and flow into the freshwater column. By maintaining constant levels in the holding tanks with suitable withdrawal rates of brine and distilled water, this configuration enables the desalination process to be run without any mechanical energy input for fluid transfer or holding the vacuum. The purpose of HE is to preheat the saline water entering the EC by the brine stream withdrawn from the EC. Fig. 1(b) shows the process schematic for a configuration utilizing low grade heat source such as thermal energy from solar collectors or process waste heat.

Fig. 2. Relation between energy, exergy and entropy transfer.

3. Exergy methodology

Traditionally, energy conversion/utilization processes have been evaluated based on the first law of thermodynamics – energy analysis. In recent times, use of exergy analysis to gain better understanding of such processes has become popular. Exergy analysis is derived from the second law of thermodynamics and provides better insights in identifying and quantifying sources of inefficiencies; selecting optimal process parameters; and in assessing resource utilization efficiency and environmental impacts.

Energy, entropy and exergy relations can be explained as shown in Fig. 2 [14]. When heat transfer occurs between two bodies from the hot side to the cold side, energy transfer takes place at the expense of thermal gradient as shown in Fig. 2. Although, an energy efficiency of 100% can be achieved between two bodies, the resultant body temperature may not be same as the source from which the heat transfer occurred. This means degradation of the energy occurred in this process of heat transfer which is often expressed as generation of entropy. As a result of entropy generation, the quality of energy transferred from the source to the sink is reduced which is reflected by the availability of energy in the sink. This degradation in the quality of energy is called exergy loss (availability loss). The exergy loss is also called irreversibility [15].

Different forms of energy have different capacities to do work. For example, potential energy, kinetic energy, and work energy can be converted completely to work, whereas, only a fraction of heat energy can be converted to work while the remainder has to be rejected to the surroundings. The property exergy serves as a measure
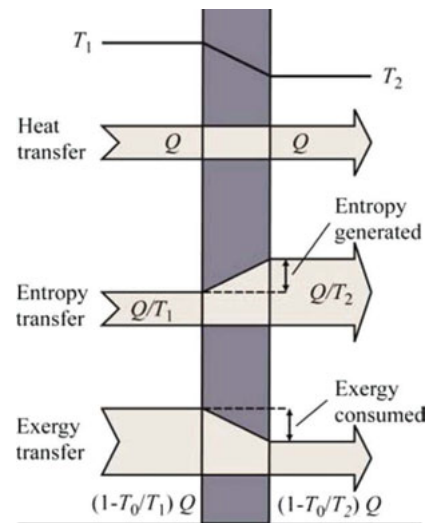
of the ability of energy to do work; it is equal to the maximum amount of work that can be extracted from a given quantity of energy. Thus, the exergy, E, associated with a given quantity of heat energy, Q, at a temperature of T can be derived from the Carnot efficiency (η_{carnot}) of a reversible heat engine working between T and the surroundings temperature, T_o:

$$E = W_{max} = \eta_{carnot}Q = \left[1 - \frac{T_o}{T}\right]Q \qquad (1)$$

From Eq. (1), the exergy factor of a given quantity of heat energy, Q can be written as:

$$\frac{E}{Q} = \left[1 - \frac{T_o}{T}\right] \qquad (2)$$

While energy is always conserved, exergy is conserved only in reversible processes. Since all real processes are irreversible, their exergy output is usually less than the exergy input. The exergy output of a process includes utilized output and unutilized output, which is the exergy flow into the environment. The total loss of exergy in a process thus includes the loss due to irreversibilities and the loss due to waste streams. Exergy analysis is carried in development and design phases and economic analysis of a system [16]. Exergy analysis plays an important role in estimating the process economics, natural resource utilization and environmental impacts of a system because the exergy performance depends on the environmental conditions (temperature and pressure) [17,18]. Other process applications

include exergy analysis of waste heat and solar energy utilization in desalination, nuclear desalination and air-conditioning systems [15,19–23].

3.1. Steady-state exergy analysis of a system

A complete steady-state analysis of energy conversion/utilization processes can be made based on mass, energy, and exergy balances. Ignoring kinetic and potential energy terms, the three conservation equations for a control volume are [24]:

Mass balance:

$$0 = \sum_i \dot{m}_i - \sum_e \dot{m}_e \tag{3}$$

Energy balance:

$$0 = \dot{Q} - \dot{W} + \sum_i (\dot{m} \cdot h)_i - \sum_e (\dot{m} \cdot h)_e \tag{4}$$

Exergy balance:

$$0 = \sum_j \left[1 - \frac{T_0}{T_j} \right] \dot{Q}_j - \dot{W} + \sum_i (\dot{m} \cdot e)_i - \sum_e (\dot{m} \cdot e)_e - \dot{E}_D \tag{5}$$

The variables are defined in the Symbols section.

While the mass and energy balance equations are well known, only the exergy balance is discussed in detail in this work. The five terms on the right hand side of the exergy equation represent the exergy associated with heat transfer, j at temperature T_j; the work transfer; the exergy inflow; the exergy outflow; and the exergy destruction, respectively. The exergy inflow and outflow associated with the streams entering and leaving the control volume are quantified in terms of the specific exergy, e, defined as follows:

$$e = (h - h_o) - T_o (s - s_o) + w(\mu - \mu_o) \tag{6}$$

For a given set of operating conditions and the corresponding properties of the working fluid, the rates of exergy destruction and exergy loss for each component of the process can be calculated from the above equations.

The following measures can now be defined to assess the thermodynamic performance of the components of a system and the entire system [24]:

Exergy destruction ratio for component c of the system, $y_{D,c}$:

$$y_{D,c} = \frac{\text{Exergy destruction in component}, \dot{E}_{D,c}}{\text{Exergy destruction in system}, \dot{E}_D} \tag{7}$$

Exergy destruction ratio for complete system, y_D:

$$y_D = \frac{\text{Exergy destruction in system}, \dot{E}_D}{\text{Exergy of fuel supplied}, \dot{E}_F} \tag{8}$$

3.2. Application of exergy method

For the purpose of this study, we focus on the following three components of the proposed desalination process: the heat exchanger HE; the evaporation chamber, EC; and the condenser, CO. The general steady-state energy and exergy balance equations (Eqs. (4) and (5)) for these three components yield the following expressions:

1. Heat exchanger, HE:

   Energy balance:

   $$0 = \dot{m}_s h_1 + \dot{m}_w h_6 - \dot{m}_s h_2 - \dot{m}_w h_7 \tag{9}$$

   Exergy balance:

   $$\dot{E}_{D,HE} = \dot{m}_s \left[(h_1 - h_2) - T_o (s_1 - s_2) + w_s(\mu_1 - \mu_2) \right] + \dot{m}_w \left[(h_6 - h_7) - T_o (s_6 - s_7) + w_w(\mu_6 - \mu_7) \right] \tag{10}$$

2. Evaporation chamber, EC:

   Energy balance:

   $$0 = \dot{Q}_{in} + \dot{m}_s h_2 - \dot{m}_w h_6 - (\dot{m}_s - \dot{m}_w) h_4 \tag{11}$$

   Exergy balance:

   $$E_{D,EC} = \left[1 - \frac{T_o}{T_3} \right] \dot{Q}_{in} + \dot{m}_s \left[\begin{array}{c} (h_2 - h_4) - T_o(s_2 - s_4) \\ + w_s(\mu_2 - \mu_4) \end{array} \right] - \dot{m}_w \left[\begin{array}{c} (h_6 - h_4) - T_o(s_6 - s_4) \\ + w_w(\mu_6 - \mu_4) \end{array} \right] \tag{12}$$

When the heat source is provided by solar energy, the Petela expression can be used to calculate the exergy of solar radiation [15]:

$$\dot{E}_s = AI_s \left[1 + \frac{1}{3} \left(\frac{T_o}{T_s} \right)^4 - \frac{4}{3} \left(\frac{T_o}{T_s} \right) \right] \tag{13}$$

3. Condenser, CO:

Energy balance:

$$0 = -Q_{\text{out}} + (\dot{m}_s - \dot{m}_w) h_4 - (\dot{m}_s - \dot{m}_w) h_5 \qquad (14)$$

where $Q_{\text{out}} = (\dot{m}_s - \dot{m}_w) \lambda_f$.

Exergy balance:

$$\dot{E}_{D,EC} = -\left[1 - \frac{T_o}{T_3}\right] \dot{Q}_{\text{out}} + (\dot{m}_s - \dot{m}_w)$$
$$\times \left[\begin{array}{c} (h_4 - h_5) - T_o (s_4 - s_5) \\ + (w_s - w_w)(\mu_4 - \mu_5) \end{array}\right] \qquad (15)$$

Energy efficiency of the desalination system is given as:

$$\text{Th}_{\text{eff}} = \frac{m_f h_v}{Q_{\text{in}}} \qquad (16)$$

This equation is also called Gained output ratio (GOR) which is less than 1 for solar powered single stage desalination system [20].

Exergy efficiency of the desalination system can be defined in two forms as shown below:

Exergy efficiency based on the latent heat (available energy or exergy) in the water vapor (steam) generated from EC:

$$\text{Ex}_{\text{eff}} = \frac{m_f h_v (1 - \frac{T_o}{T})}{Q_{\text{in}}} \qquad (16a)$$

Overall exergy efficiency based on available energy or exergy in the freshwater condensed in condenser (final product):

$$\text{Ex}_{\text{eff}} = \frac{m_f \left\{ (h_5 - h_o) - T_o (s_5 - s_o) \right\}}{Q_{\text{in}}} \qquad (16b)$$

This equation is based on the available energy (exergy) in the water vapor generated from EC.

The environmental references for the exergy analysis were taken as temperature, 25°C (298 K), and salt concentration of 3.5%.

4. Results and discussion

4.1. Temperature and freshwater production profiles

The experimental studies were conducted during summer season at the Engineering Research Facility (ERF) of New Mexico State University in Las Cruces,

New Mexico, USA. The solar insolation varied between 400 and 1100 W m⁻² while the ambient temperatures ranged 15–35°C during these experiments. The maximum ambient temperature recorded was 35°C while the maximum temperature of the brackish water in the EC was 52.75°C. As a comparison, the maximum saline water temperatures measured for different configurations were as follows: low temperature process using direct solar energy (SS configuration – SSV) 50°C, low temperature process using direct solar energy fitted with an external reflector (SS configuration (SSR) 53°C and low temperature process using solar energy as well as photovoltaic energy (SSP) 55°C respectively (Fig. 3(a)). This configuration is referred as SSPV during non-sunlight hours when the photovoltaic energy is utilized for evaporation. These temperatures are lower than those commonly reported for a SS that are in the range: 60–75°C [7,8].

Daily freshwater production rates for the different configurations are shown in Fig. 3(b). The low temperature desalination process as a SS configuration
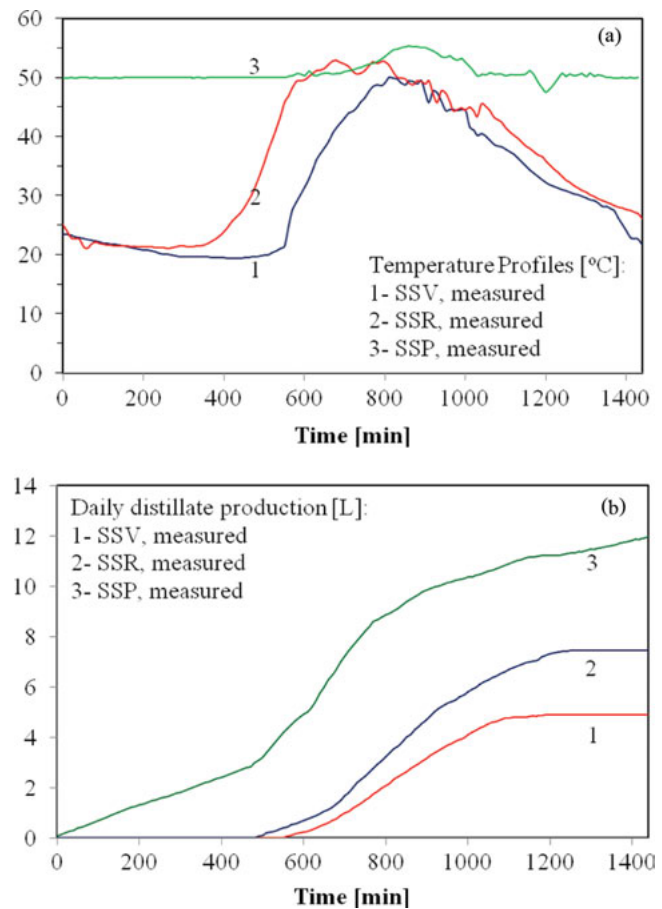

Fig. 3. Temperature (a) and freshwater (b) profiles of the low temperature desalination system for different configurations.

(SSV) produces freshwater of about 5 l d⁻¹ m⁻², nearly 1.5–2 times that of typical SS [7,8]. This improvement can be attributed to the reduction in energy losses by the low temperature desalination process. The near-vacuum pressures created by natural means of gravity and barometric head allow for the evaporation of freshwater to occur at low temperatures resulting in higher energy efficiency. This configuration, when fitted with a reflector SSR produced about 7.5–8 l d⁻¹ m⁻² of distillate which is three times that of a typical SS. As the solar insolation incident on the SS was intensified by the reflector, the saline water temperatures rose quickly resulting in evaporation of freshwater as shown in Fig. 3(a). The low temperature process powered by photovoltaic energy SSP produced over 12 l d⁻¹ when fitted with a reflector. Photovoltaic area required for this configuration was 6 m². Photovoltaic energy generated during the day is sufficient to produce freshwater of 4–5 l d⁻¹ during the night time. The efficiency of the PV modules is 14%. The process can be designed to operate round the clock with a backup external heat source such as thermal energy storage tank when solar energy is not available.

4.2. Energy analysis of solar powered desalination system

Fig. 4(a) shows the solar energy utilization patterns of the low temperature desalination process for the SSV, SSR, SSP and SSPV configurations. The entire solar energy incident on the EC is not used for evaporation. Incident solar energy passes through the glass top (some reflected back) and is absorbed by the saline water (about 89%). Total solar energy, energy available after optical losses, energy utilized for freshwater production and the useful latent heat in the product are shown for each of the configurations. For the SSV experimental set, the total amount of solar energy available was 21.6 MJ which is equal to 6 kWh m⁻² d⁻¹. About 19.2 MJ (89%) of the total solar energy was available for conversion into thermal energy after optical losses. Out of this available solar energy, 12.1 MJ (63%) was utilized for evaporation of freshwater of 5.25 l from saline water after the heat losses from the evaporation chamber and condenser to the surroundings (Fig. 4(a)). Traditional SS have a thermal efficiency of about 30% and rarely exceed 45% [7,8]. Normal SS operating with an efficiency of 45%, will require 5040 kJ of thermal energy per kg of freshwater produced. The proposed process SSV operates at higher thermal efficiencies with a specific energy consumption of 3900 kJ kg⁻¹ of freshwater. Incident solar energy available for SSR experimental set was 24.1 MJ (6.7 kWh m⁻² d⁻¹). About 21.4 MJ of solar energy has passed through the glass cover and the saline water body to cause evaporation. Out of this
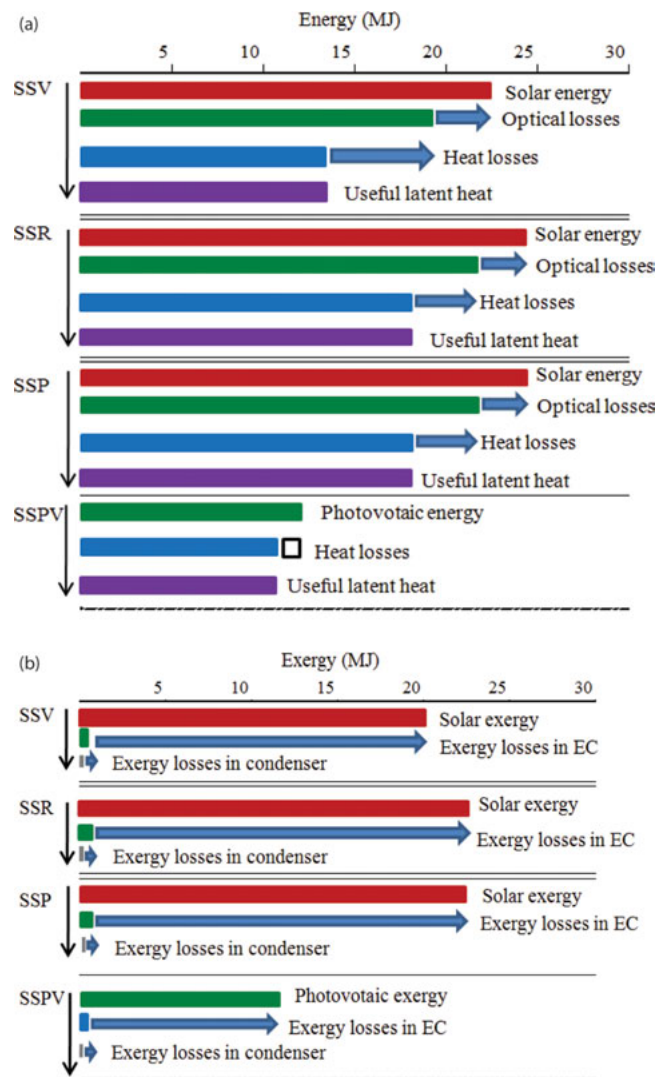

Fig. 4. Energy analysis (a) and exergy analysis (b) of the low temperature desalination system using direct solar and photovoltaic energy.

available energy, 17.3 MJ was utilized to produce freshwater. Thermal efficiency of SSR was between 70% and 80% with a specific energy consumption of 3200 kJ kg⁻¹. The specific energy required for the configuration with photovoltaic energy SSP is only 2800–3000 kJ kg⁻¹ of freshwater with thermal efficiencies ranging between 80% and 90%. In the case of traditional SS and SSV, major energy losses occur through the glass cover during sunlight hours. However, for SSPV (SSP during non-sunlight hours), the glass cover can be covered with insulation during non-sunlight hours to reduce the energy losses to the ambient. Additionally, lower ambient temperatures during non-sunlight hours favor the convection and condensation of freshwater vapors from the evaporation chamber to the condenser side [3].

4.3. Exergy analysis of solar powered desalination system

The solar exergy utilization patterns of the low temperature desalination process for SSV, SSR, SSP configurations are shown in Fig. 4(b). Total available solar exergy available after optical losses, exergy utilized (exergy losses in the evaporation chamber) for freshwater production and the exergy losses in the condenser (due to latent heat dissipation) and exergy available in the product are shown for each of the configurations. In few studies, the solar exergy value is taken same as the energy value, given that the temperature of the sun is very high in relation to the ambient temperature [25]. In this study we used the Petela equation to account for actual solar exergy value [15]. Available solar exergy for SSV configuration was 20.1 MJ. Although, some portion of this exergy was utilized to evaporate freshwater, the exergy losses in the evaporation chamber were 19.2 MJ. The exergy available in the latent heat of the freshwater vapor was 0.9 MJ. Finally, exergy available in the condensed water vapor (freshwater) was only 0.008 MJ. Thus, exergy efficiency of the SSV process configuration was around 0.04% (using Eq. (16b)). If the exergy associated with the water vapor is considered, the exergy efficiency of the SSV process configuration was 4.6% indicating the efficiency of the evaporation chamber (using Eq. (16a)). For SSR configuration, the solar exergy was 22.5 MJ. The exergy losses in the evaporation chamber were 20.9 MJ. The exergy available in the latent heat of the freshwater vapor was 1.6 MJ. Finally, exergy available in the condensed water vapor (freshwater) was only 0.012 MJ. Thus, exergy efficiency of the SSR process configuration was around 0.05% (using Eq. (16b)). Since, this is a single stage configuration, if the exergy associated with the water vapor is considered, the exergy efficiency of the SSR process configuration was 7.0% which is the efficiency of the evaporation chamber (using Eq. (16a)).

Although, energy efficiency of the photovoltaic powered process was higher (90%) than other configurations, the exergy efficiency was lower than other configurations (0.039%, using Eq. (16b)). This is due to high exergy value (=1) of electrical energy generated by the photovoltaic modules. Therefore, it is clear that high quality form of energy is not appropriate for desalination process due to enormous quantities of exergy destruction in the condenser. However, the exergy efficiency can be slightly improved in a multi-effect configuration. A recent study incorporated solar collectors to provide heat source to the flash chamber at low pressures [26]. The reported first law efficiency was 19%. Exergy efficiency of the system varied between 15% and 26% when the solar radiation ranged from 400 to 900 W m⁻² considering energy harvested in the solar collectors. Freshwater production rate of 8.5 l d⁻¹ was obtained

with a solar collector area of 2 m². Although the operating principle was very similar to this process (vacuum created by a pump and varied between 0.05–1 bar), the solar energy was harvested by the circulating fluid in the solar collector as such the solar exergy was supplied to the inlet saline water (circulating fluid inlet and outlet temperatures were 20°C and 80°C respectively) with exergy recovery from the condenser whereas in the proposed process the solar exergy was directly utilized in the evaporation chamber for evaporation of freshwater from the saline water at around 50°C with no energy recovery from the condenser. Another study reported the performance of triple effect distiller powered by solar energy. Single effect, double effect and triple effect efficiencies were recorded as 4%, 17–20% and 19–26% respectively. High exergy efficiencies are due to energy recovery between the stages [27]. If exergy losses can be recovered from the condenser, the exergy performance of the proposed process can be further improved.

4.4. Exergy analysis using low grade heat source

When a low grade heat source was utilized to run the low temperature desalination process, freshwater production rate of 0.250 kg h⁻¹ was obtained (Fig. 1(b)). The withdrawal rate was fixed at 0.250 kg h⁻¹, while the heat source temperature was 60°C. The amount of concentrated saline water removed from evaporation chamber to maintain the salt concentration is defined as withdrawal rate. Temperature, enthalpy, and entropy values for different process state points are shown in Table 1a. The heat source in the heat exchanger entered at 60.1°C and exited at 50.3°C at a flow rate of 19 kg h⁻¹. Thermal energy efficiency of the evaporation chamber was around 75%. The main process components are the heat exchanger # 1, evaporation chamber and condenser. The exergy inputs and outputs from individual process components are shown in Table 1b. Exergy destruction (loss %), irreversibility and second law efficiencies are shown for the process components. It can be seen that heat exchanger #1 operates at close to 20% exergy efficiency even though its energy efficiency was around 80%. However, it should be noted that the amount of exergy loss is very small compared the exergy losses in the evaporation chamber and condenser. The exergy loss in the evaporation chamber is 40.61% (29.39 kJ h⁻¹) and the exergy loss in the condenser is 98.69% (42.43 kJ h⁻¹). From this analysis, it can be concluded that the highest quantity of exergy loss occurs in the condenser in the form of latent heat dissipation from the water vapor to the environment. Overall exergy efficiency of the process is 0.78% (using Eq. (16b)) which is higher than the process configurations utilizing direct solar and photovoltaic energy.

Table 1a
Exergy parametric values at different state points of the low temperature desalination system

Process point	1	2	3	4	5	6	7
Phase	Liquid	Liquid	Liquid	Vapor	Liquid	Liquid	Liquid
Temperature (°C)	25	32	49.4	49.1	40.4	49.4	34
Pressure (kPa)	0	0	11.9	11.8	7.2	0	0
Mass flow rate (kg h^{-1})	0.5	0.5	0.5	0.25	0.25	0.25	0.25
Sp. entropy (kJ kg^{-1} °C^{-1})	0.35	0.48	0.67	0.64	0.54	0.66	0.48
Sp. enthalpy (kJ kg^{-1})	100	128	198	2300	160	196	136
Chemical exergy (kJ kg^{-1})	70.8	73.2	80.5	−20.3	−14.5	80.5	73.8
Sp. flow exergy (kJ kg^{-1})	0.2	0.4	4	4	1.5	4	0.5
Exergy factor (1-T$_o$ T^{-1})	0	0.023	0.076	0.075	0.049	0.076	0.029

Table 1b
Exergy analysis for individual components of the desalination system powered by low grade heat source

Process component	Exergy input E_{in} (kJ h^{-1})	Exergy output E_{out} (kJ h^{-1})	Irreversibility I (kJ h^{-1})	Exergy loss (%)	Second law efficiency Ψ (%)
Heat exchanger	0.85	0.17	0.68	80.12	19.88
Evaporation chamber	72.38	42.99	29.39	40.61	59.39
Condenser	42.99	0.56	42.43	98.69	1.31

When a multi-effect configuration is considered, the exergy efficiency of the process may not improve significantly since the final product from the process is freshwater in its liquid form. The exergy efficiency of a MSF process has been reported to be 4% with 22 flash stages and that of solar powered (solar collectors) MED process as 14.3% with 14 stages while the second law efficiencies of membrane distillation and humidification-dehumidification processes are 0.5% and 5.7% respectively [28–31]. Exergy efficiencies of low specific energy consuming processes such as reverse osmosis (RO), nanofiltration (NF) and electrodialysis (EDR) processes have been reported to be only around 8%, 9.7% and 6.3% respectively [32–35]. The above mentioned studies may have considered different process parameters and environmental references pertinent to each study; however in fundamental interest, it is clear that the exergy is lost in any thermally operated system and thermal desalination process is an irreversible process. Therefore, since exergy destruction in the desalination process is inevitable, it is wise to utilize low grade (in other words, low exergy) heat sources to run the desalination process while high quality electrical and mechanical energies can be utilized in high efficiency (thermodynamically efficient) processes. Since freshwater is required in large quantities, it is not thermodynamically efficient to use high quality (high exergy) heat sources even if they are available at a reasonable cost. This study is based on the amounts of thermal exergy provided to the desalination system and that recovered from the desalination system. However, if a different route were chosen to conduct desalination using chemical exergy in the sea or brackish waters and recover the chemical exergy in the brine stream, such a process may result in improved overall exergy efficiency of the desalination system.

5. Conclusions

Energy and exergy performance of a low temperature desalination process utilizing direct solar energy, photovoltaic energy and low grade heat source was presented. It was observed that the overall exergy efficiency of the desalination process was very low. For the single stage operation of the low temperature desalination process, the overall exergy efficiencies were 0.04%, 0.051%, and 0.039% respectively for SSV, SSR, and SSP configurations. For the system utilizing low grade heat source, the exergy efficiencies were 59.39%, 19.88%, and 1.31% for heat exchanger, evaporation chamber, and condenser respectively. The overall exergy efficiency of the process was 0.78%. The greatest amount of exergy

destruction occurred in the condenser for this process. The exergy efficiency of the evaporation chamber for the low grade heat source was higher than solar energy and photovoltaic energy sources. This study indicates that utilizing low grade heat sources such as process waste heat can result in higher energy and exergy efficiencies and improve the economics of the desalination process while thermal and electrical energy harvested from the solar energy can be utilized in energy and exergy efficient processes such as an air-conditioning system and power generation cycles since the exergy value of the solar energy is high.

Acknowledgements

Symbols

c_p	—	specific heat of ideal gas at constant pressure (kJ kg^{-1} K^{-1})
E	—	exergy (kJ)
$\dot{E}$	—	exergy flow rate (kW)
h	—	specific enthalpy (kJ kg^{-1})
$\dot{m}$	—	mass flow rate (kg h^{-1})
p	—	pressure (atm.)
Q	—	heat energy (kJ)
$\dot{Q}$	—	total heat transfer rate (kW)
s	—	specific entropy (kJ kg^{-1} K^{-1})
T	—	absolute temperature (K)
T_o	—	reference temperature (K)
$\dot{W}$	—	net work transfer rate (kW)
w	—	seawater concentration (kg kg^{-1})

Greeks

Ψ	—	exergetic efficiency (%)
μ	—	chemical exergy (kJ kg^{-1})
η	—	thermal efficiency (%)

Subscripts

D	—	destruction
e	—	exit, specific exergy
i	—	inlet
in	—	input, supply
o	—	surroundings
s	—	saline water stream, sun
th	—	thermal
w	—	withdrawal stream

References

[1] V.G. Gude, N.N. Khandan and S. Deng, Renewable and sustainable approaches for desalination, Renewable Sustainable Energy Rev., 14 (2010) 2641–2654.
[2] R. Semiat, J. Sapoznik and D. Hasson, Energy aspects in osmotic processes, Desalin. Water Treat., 15 (2010) 228–235.
[3] S. Al Kharabsheh and D.Y. Goswami, Analysis of an innovative water desalination system using low-grade solar heat, Desalination, 156 (2003) 323–332.
[4] R. Balan, J. Chandrasekaran, S. Shanmugan, B. Janarthanan and S. Kumar, Review on passive solar distillation, Desalin. Water Treat., 28 (2011) 217–238.
[5] T.V. Arjunen, H.S. Aybar and N. Nedunchezhian, Effect of sponge liner on the internal heat transfer coefficients in a simple solar still, Desalin. Water Treat., 29 (2011) 271–284.
[6] C. Park, B. Lim and K. Chung, Experimental results of a seawater distiller utilizing waste heat of a portable electric generator, Desalin. Water Treat., 31 (2011) 134–137.
[7] S.A. Zeinab and A. Lasheen, Experimental and theoretical study of a solar desalination system in Cairo, Egypt, Desalination, 217 (2007) 52–64.
[8] A.E. Kabeel, Performance of solar still with a concave wick evaporation surface, Energy, 34 (2009) 1504–1509.
[9] V.G. Gude and N.N. Khandan, Desalination at low temperatures and low pressures, Desalination, 244(1–3) (2009) 239–247.
[10] V.G. Gude, N.N. Khandan and S. Deng, Integrated PV-thermal system for desalination and power production, Desalin. Water Treat., 36 (2011) 129–140.
[11] V.G. Gude, N.N. Khandan and S. Deng, Desalination using solar energy: Towards sustainability, Energy, 36(1) (2011) 78–85.
[12] V.G. Gude, N.N. Khandan and S. Deng, Integrated PV-thermal system for desalination and power production, Desalin. Water Treat., 36 (2011) 129–140.
[13] V.G. Gude and N.N. Khandan, Desalination using low-grade heat sources, ASCE J. Energ. Eng., 134 (3) (2008) 95–101.
[14] B. Sandnes, Exergy Efficient Production, Storage and Distribution of Solar Energy, Ph.D. Dissertation, University of Oslo, November 2003.
[15] A. Hepbasli, A key review on exergetic analysis and assessment of renewable energy resources for a sustainable future, Renewable Sustainable Energy Rev., 12 (2008) 593–661.
[16] A. Martinez, J. Uche, C. Rubio and B. Carrasquer, Exergy cost of water supply and water treatment technologies, Desalin. Water Treat., 24 (2010) 123–131.
[17] A.A. Mabrouk, A.S. Nafey and H.E.S. Fath, Steam, electricity and water costs evaluation of power-desalination co-generation plants, Desalin. Water Treat., 22 (2010) 56–64
[18] Y.A. Gogus, U. Camdali and M.S. Kavsaoglu, Exergy balance of a general system with variation of environmental conditions and some applications, Energy, 27 (2002) 625–46.
[19] S. Nisan, Utilisation of the exergy method for the cost evaluation of integrated nuclear desalination systems, Desalin. Water Treat., 8 (2009) 225–235.
[20] G.P. Narayan, M.H. Sharqawy, J.H. Lienhard and S.M. Zubair, Thermodynamic analysis of humidification–dehumidification desalination cycles, Desalin. Water Treat., 16 (2010) 339–353.
[21] A. Ucar and M. Inalli, Thermal and exergy analysis of solar air collectors with passive augmentation techniques, Int. Commun. Heat Mass Transfer, 33 (2006) 1281–1290.
[22] K.H. Mistry, J.H.V. Leinhard and S.M. Zubair, Effect of entropy generation on the performance of humidification–dehumidification desalination cycles, Int. J. Therm. Sci., 49 (2010) 1837–47.
[23] J. Siqueiros and F.A. Holland, Water desalination using heat pumps, Energy, 2000, 717–729.
[24] A. Bejan, G. Tsatsaronis and M. Moran, Thermal design and optimization, John Wiley & Sons, New York, 1996.
[25] J.J. Navarrete-González and J.G. Cervantes-de Gortari, Exergy analysis of a rock bed thermal storage system, Int. J. Exergy, 5(1) (2008) 18–30.

[26] J. Joseph, R. Saravanan and S. Renganarayanan, Studies on a single-stage solar desalination system for domestic applications, Desalination, 173 (2005) 77–82.

[27] O. Sow, M. Siroux and B Desmet, Energetic and exergetic analysis of a triple-effect distiller driven by solar energy, Desalination, 174 (2005) 277–286.

[28] Y. Cerci, Y. Cengel, B. Wood, N. Kahraman, and E. Karakas, Improving the thermodynamic and economic efficiencies of desalination plants: Minimum work required for desalination and case studies of four working plants. Desalination and water purification research and development program final report No. 78, U.S. Department of the interior, November 2003.

[29] L. García-Rodríguez and C. Gómez-Camacho, Exergy analysis of the SOL-14 plant (Plataforma Solar de Almería, Spain), Desalination, 137 (2001) 251–258.

[30] F. Banat and N. Jwaied, Exergy analysis of desalination by solar-powered membrane distillation units, Desalination, 230 (2008) 27–40.

[31] S. Hou, D. Zeng, S.Ye and H. Zhang, Exergy analysis of the solar multi-effect humidification-dehumidification desalination process, Desalination, 203 (2007) 403–409.

[32] N. Kahraman, Y.A. Cengel, B. Wood and Y. Cerci, Exergy analysis of a combined RO, NF, and EDR desalination plant, Desalination, 171 (2004) 217–232.

[33] I.H. Aljundi, Second-law analysis of a reverse osmosis plant in Jordan, Desalination, 239 (2009) 207–215.

[34] Y. Cerci, Exergy analysis of a reverse osmosis desalination plant in California, Desalination, 142(3) (2002) 257–266.

[35] H. Mehdizadeh, Membrane desalination plants from an energy-exergy viewpoint, Desalination, 191 (2006) 200–209.